Journal of Controlled Release 156 (2011) 85–91

Contents lists available at ScienceDirect

Journal of Controlled Release

journal homepage: www.elsevier.com/locate/jconrel

NANOMEDICINE

Combined MUC1-specific nanobody-tagged PEG-polyethylenimine polyplex targeting and transcriptional targeting of tBid transgene for directed killing of MUC1 over-expressing tumour cells

Elham Sadeqzadeh [a], Fatemeh Rahbarizadeh [a,*], Davoud Ahmadvand [b], Mohammad J. Rasaee [a], Ladan Parhamifar [b], S. Moein Moghimi [b]

[a] Department of Medical Biotechnology, Faculty of Medical Sciences, Tarbiat Modares University, Tehran, Iran
[b] Center of Pharmaceutical Nanotechnology and Nanotoxicology, University of Copenhagen, Universitetsparken 2, DK-2100 Copenhagen Ø, Denmark

ARTICLE INFO

Article history:
Received 6 March 2011
Accepted 10 June 2011
Available online 24 June 2011

Keywords:
Cancer nanomedicines
MUC1
Nanobody
Poly(ethylene glycol)
Polyethylenimine
Transcriptional targeting

ABSTRACT

We provide evidence for combining a single domain antibody (nanobody)-based targeting approach with transcriptional targeting as a safe way to deliver lethal transgenes to MUC1 over-expressing cancer cells. From a nanobody immune library, we have isolated an anti-DF3/Mucin1 (MUC1) nanobody with high specificity for the MUC1 antigen, which is an aberrantly glycosylated glycoprotein over-expressed in tumours of epithelial origin. The anti-MUC1 nanobody was covalently linked to the distal end of poly(ethylene glycol)$_{3500}$ (PEG_{3500}) in PEG_{3500}-25 kDa polyethylenimine (PEI) conjugates and the resultant macromolecular entity successfully condensed plasmids coding a transcriptionally targeted truncated-Bid (tBid) killer gene under the control of the cancer-specific MUC1 promoter. The engineered polyplexes exhibited favourable physicochemical characteristics for transfection and dramatically elevated the level of Bid/tBid expression in both MUC1 over-expressing caspase 3-deficient (MCF7 cells) and caspase 3-positive (T47D and SKBR3) tumour cell lines and, concomitantly, induced considerable cell death. Neither transgene expression nor cell death occurred when the MUC1 promoter was replaced with the CNS-specific synapsin I promoter. Since PEGylated PEI was only responsible for DNA compaction and played no significant role in direct transfection and cell killing, our attempts overcome previously reported PEI-mediated apoptotic and necrotic cell death, which is advantageous for future *in vivo* transcriptional targeting as this will minimize (or eliminate) non-targeted cell damage.

1. Introduction

Cancer gene therapy is at the forefront of therapeutic research and has the advantage that normal tissue toxicity might be avoided if suitable strategies can be used to target the therapeutic transgenes directly to cancer cells [1–3]. A promising approach in cancer gene therapy is exploitation of the natural killing ability of proapoptotic genes such as the BH3-only proteins [4,5]. A selected example is Bid that acts as a sentinel for protease activation (caspase-8, caspase-3, granzyme B, calpain, cysteine cathepsins and cathpesin D) resulting from different stimuli and cellular injuries [6–8]. Cytosolic p22 Bid when activated by limited proteolysis in the loop region generates p15 Bid or truncated-Bid (tBid) [9]. tBid translocates to the mitochondria through a process facilitated by the mitochondrial carrier homologue2/Met-induced mitochondrial protein [10]. Bid cleavage also exposes its N-terminal BH3 domain; this interacts with pro-apoptotic proteins Bax and Bak assisting their oligomerization and inducing mitochondrial outer membrane permeabilization, which leads to cytochrome *c* release, subsequent apoptosome assembly and activation of caspases 9, 3 and 7 [11].

Since Bid activity is tightly regulated by post-transcriptional modification and sub-cellular localization, transcriptional targeting has been introduced to direct tBid expression specifically to cancer cells [4,5]. Indeed, tBid is an ideal killer transgene candidate; it has a small size and does not require post-translational modification. Transcriptional targeting utilizing tissue-specific promoters exploits genes that are switched on only in certain tissues or diseased states [3]. In this respect, we have recently designed an effective hybrid promoter consisting of two response modules (hypoxia responsive elements and estrogen response elements, which are activated by microenvironmental settings) and the MUC1 promoter for transcriptional targeting of tBid to breast cancer cells, resulting in effective MUC1-positive cell killing [4]. Indeed, the MUC1/DF3 gene encodes a high molecular weight mucin-like glycoprotein, which is predominantly over-expressed at the transcriptional level in tumours of epithelial origin such as breast and colon [12,13].

* Corresponding author at: Department of Medical Biotechnology, Faculty of Medical Sciences, Tarbiat Modares University, Tehran, Iran. P.O. Box: 14115-331. Tel.: +98 21 82883884; fax: +98 21 82884555, +98 21 82884526.
E-mail address: Rahbarif@modares.ac.ir (F. Rahbarizadeh).

0168-3659/$ – see front matter © 2011 Elsevier B.V. All rights reserved.
doi:10.1016/j.jconrel.2011.06.022

As well as controlled regulation of transgene expression, controlling the delivery of the therapeutic gene to tumour tissue remains pivotal. We have now extended our studies to address this issue. Our approach is based on the design of non-viral vectors utilizing poly (ethylene glycol) (PEG)-polyethylenimine (PEI) conjugates tagged with a newly derived tumour-specific single domain antibody (nanobody). PEI is a polycation that exhibits a strong proton buffer capacity over a broad pH-range [14]. Accordingly, PEI is not only capable of condensing nucleic acids into nanostructures (polyplexes) with a high cationic surface charge, but also allowing sufficient gene transfer without endosome disruptive reagents. Excellent transfection results have been reported with 25 kDa branched PEI polyplexes, however, due to their high cationic surface charge the effect remains cell non-specific [14,15]. Although being amongst the most prominent and effective non-viral nucleic acid delivery systems, the 25 kDa branched PEI is highly cytotoxic and induces necrotic and apoptotic cell death in a concentration- and cell type-dependent manner [16,17]. Functionalization of PEI with PEG overcome these hurdles considerably; sufficient PEGylation leads to generation of vectors with a surface charge close to neutrality (through surface shielding effect of PEG), far lower levels of non-specific interactions and cytotoxicity [14,18,19]. Furthermore, PEGylation suppresses macrophage clearance and prolongs circulation times of intravenously injected vectors, which is necessary for polyplex extravasation into solid tumours to enable efficient systemic delivery of transgenes [20,21]. To overcome the steric barrier of surface-projected PEG molecules in polyplex for uptake by target cells, we have isolated a new anti-MUC1 single domain antibody (V_{HH} fragment or nanobody) with high specificity for the MUC1 antigen from a nanobody immune library, and attached this to the distal end of the PEG in PEI-PEG conjugates. Nanobodies are beginning to expand the repertoire of antibody-based reagents attractive for cancer targeting [22,23]; they are of small size, mostly nonimmunogenic, exhibit very high affinity for their corresponding antigens and are highly stable over broad temperature and pH ranges, which make them amenable for conjugation procedures. Our described work provides the *in vitro* proof of concept in combining a nanobody-based targeting approach with transcriptional targeting as a safe way to deliver lethal transgenes specifically to tumour cells.

2. Materials and methods

2.1. Materials

Synthetic mucin peptide, TSA-P1-24 (TSAPDTRPAPGSTAPPAHGVTSAPDTR), corresponding to the mucin core protein, was chemically conjugated to bovine serum albumin (BSA) by reaction with glutaraldehyde (TSA-P1-24-BSA) [24]. Monoclonal anti-hemagglutinin (anti-HA) conjugated to horseradish peroxidase (HRP) and HRP conjugated anti C-myc were obtained from Roche (Mannheim, Germany). HRP-conjugated anti-M13 was purchased from Amersham Pharmacia Biotech AB (Uppsala, Sweden). FITC conjugated rabbit anti-mouse antibody was purchased from LifeSpan BioSciences (Seattle, WA). Heterobifunctional poly(ethylene glycol)$_{3500}$, succinimidyl-([*N*-maleimidopropionamido]-poly(ethylene glycol) ester (Mal-PEG$_{3500}$-NHS), was purchased from JenKem Technology (Beijing, China). All other reagents used in this study were of analytical grade and were purchased from Sigma Chemical Co. (St. Louis, MO, USA). The native cancerous MUC1 was purified from ascitic fluid of a patient with aggressive small-cell lung carcinoma with metastasis to the peritoneum as described before [25].

2.2. Bacterial strains and media composition

Escherichia coli TG1 (Pharmacia, Uppsala, Sweden) were used as host for phagemid manipulation and antibody high expression. *E. coli* Rosetta-Gami 2 (Novagen, Madison, WI) was used for soluble antibody production.

Luria–Bertani (LB) and super broth (SB) media, supplemented with 150 μg/mL ampicillin were used for the selection of transformants. LB medium, supplemented with 0.01 M $MgCl_2$ and 0.02 M glucose was the media of choice for electroporation and M9-medium supplemented with ampicillin (150 μg/mL) and IPTG (1 mM) were used as expression media.

2.3. Cell lines and culture conditions

The cell lines used in this study were chosen from cells with different levels of human MUC1 expression. MCF7 (human breast adenocarcinoma cell line), T47D (human ductal carcinoma cell line) and SKBR3 (human breast adenocarcinoma cell line) were used as models with high expression of MUC1. A431 (human squamous cell carcinoma of head and neck cell line, with limited expression of MUC1) and NIH3T3 (fetal murine fibroblast like cell line, with no expression of MUC1) represented controls [12,13,25]. The cells were cultured in DMEM or RPMI supplemented with 10% fetal bovine serum (FBS), penicillin (100 IU/mL) and streptomycin (100 μg/mL). All cells were grown at 37 °C in a humidified 5% CO_2 atmosphere.

2.4. Gene constructs containing transcriptionally targeted killer gene

tBid gene was amplified by PCR on peripheral lymphocytes cDNA, and cloned in the pCDNA3.1/Hygro$^+$ (Invitrogen, Carlsbad, CA). An oligomer containing three copies of a hypoxia response element (HRE) and two copies of estrogen response elements (ERE) were designed (3HRE/2ERE), amplified and cloned upstream of the tBid in the same vector. The MUC1 promoter (pMUC1) was also amplified by PCR on lymphocyte genomic DNA and cloned in the construct downstream of the response elements and upstream of the tBid gene. Detailed procedures for preparation and functional confirmation of the final product, pCDNA-3HRE/2ERE-pMUC1-tBid, was previously described by us [4]. For design of the tBid control vector, we replaced the 3HRE/2ERE-pMUC1 with the repressor element 1 (RE1)-RE1-RE1-pSyn (synapsin I promoter) [26]. A Green Fluorescent Protein (GFP) construct (pCDNA3.1-Hygro$^+$-GFP under the control of CMV promoter) was also used.

2.5. Library construction, panning and isolation of anti-MUC1 nanobody

Total RNA from peripheral blood lymphocytes of TSA-p1-24 peptide immunized *Camelus dromedaries*, was isolated (Qiagen RNA purification kit, Qiagen, Valencia, CA, USA) and used as a template for cDNA synthesis (Roche). DNA Fragments encoding nanobodies were amplified by nested PCR and all other procedures for the preparation of a phagemid nanobody gene library were described in detail elsewhere [27].

Five rounds of selections were performed using biopanning on antigen coated microplate. The 12-well plate (Wallach, Gaithersburg, MD) was coated with MUC1 whole molecule, purified from ascetic fluid (0.2 and 0.6 μg/mL). The same concentrations of BSA in phosphate buffer saline (PBS) were used as negative control. On the other hand, phage particles of immune library were produced by rescue with helper phage M13K07 (Amersham-Pharmacia-Biotech). Phages were concentrated using PEG-NaCl (20 g/L and 2.5 M, respectively), eluted in 500 μL of 4% skimmed milk in PBS (4% MPBS), added to coated wells and incubated for 1 h at 37 °C. Wells were then washed five times with PBS-Tween 20 (0.1%, 0.3%, 0.5%, 1% and 2% in five consecutive rounds) followed by 10 times washing with PBS. Bound phages were then eluted with 100 mM of triethylamine, neutralized after 10 min with Tris–Cl (1 M, pH 7.4) and added to 10 mL of TG1 ($A_{600nm} = 0.8$) grown at 37 °C. The accuracy of five rounds of panning was confirmed by sequencing of some randomly

selected clones and polyclonal phage ELISA using anti-M13-HRP [28]. The product of fifth round of panning was transformed to *Rosetta-gami 2*. Randomly selected clones were cultured overnight and checked by ELISA using anti-HA-HRP. DNA sequence of the selected clone (ER-46) was confirmed by sequencing.

2.6. Over-expression and purification of anti-MUC1 nanobody

The selected nanobody gene was sub-cloned in pSJ expression vector, which fuses the C-myc-tag and His-tag to the end of the nanobody, using primers flanked with *Bam*H1 and *Bpu*A1 restriction sites (Table 1).

Reverse primer added a cysteine amino acid at the C-terminal of nanobody protein. The construct was electroporated into TG1. The final clone (ER46-28) was selected by colony-PCR and confirmed by sequencing. The cultures were induced with different concentrations of IPTG (0.5, 0.8, and 1 mM) in various conditions of induction time and temperature (16, 36, and 72 h and 28, 32, and 37 °C, respectively).

Bacterial culture in the best condition in M-9 expression media containing casamino acid was performed for large scale production of nanobody. Anti-MUC1 nanobody was purified from the periplasm extract using immobilized metal affinity chromatography (IMAC) (Qiagen, Hilden, Germany) according to the manufacturer's protocol and eluted with 200 mM imidazole. Purification was confirmed by SDS-PAGE and immunobloting (under reduced conditions and the blotting was performed using antiC-myc antibody). Protein content was measured by Bradford assay [29].

2.7. Reactivity of nanobody

2.7.1. Enzyme Linked Immunosorbent Assay (ELISA)

The reactivity of the purified antibody was tested against purified MUC1 antigen from cancerous sources (2 ng/mL) and BSA (100 ng/mL) (as a negative control) by ELISA as described in detail earlier [24]. Bound nanobody was detected with 1:2000 diluted anti-C-myc-HRP. The affinity of nanobody was determined as described by Beaty and Beaty [30].

2.7.2. Radioimmunoassay

The ER46-28 nanobody was labeled using the chloramin-T method. Briefly, 10 μg of anti-MUC1 nanobody in 25 μL PBS (0.5 M, pH 7.5) was added to 7.4 MBq of $Na^{131}I$. Then 25 μL of freshly made chloramin-T (2 mg/mL) was added and the mixture incubated for 0.5 min at room temperature. The reaction was stopped by adding 2.4 mg/mL sodium metabisulfite, 10 mg/mL tyrosine and 10% glycerol, in PBS. The unbound $Na^{131}I$ was separated from the labeled antibody by gel-filtration chromatography (Sephadex-G25). The reactivity of radiolabelled ER46-28 (0.2 μg/well) against purified MUC1 antigen, TSA-P1-24-BSA and BSA was measured. The antigen coated wells were washed and blocked with 2% gelatin in PBS (10 mM, pH 7.2) for 1 h at 37 °C. At the end of incubation time, wells were washed and challenged with 30,000 cpm of [^{131}I]-nanobody and incubated at 37 °C for 1 h. The content of the wells were emptied, wells were then washed and the radioactivity in the wells was measured by a Perkin Elmer gamma counter.

Table 1
List of PCR primers.

Primer	DNA sequence
Nano-BbsI	5′-TATGAAGACACCAGGAGGTGCAGCTGGAGCAGTC-3′
Nano-BamH-cys	5′-TATGGATCCGCATGAGGAGACGGTGACCTG-3′
For-beta-act	5′-TCCCTGGAGAAGAGCTACG-3′
Rev-beta-act	5′-GTAGTTTCGTGGATGCCACA-3′
For-bid-Real	5′-GGCTTCCTCCAAAGCTGTTCTG-3′
Rev-bid-Real	5′-GATGATGTCTTCTTGACTTTC-3′

2.7.3. Cell ELISA

The reactivity of anti-MUC1 nanobody with both MUC1 positive (MCF7, T47D and SKBR3) and negative (NIH3T3) cell lines was also tested. Cells were grown in sterile 96-well culture microtiter plates in RPMI-1640 (Sigma) supplemented with 10% v/v foetal bovine serum, penicillin (100 U/mL) and streptomycin (100 μg/mL) until confluent. The supernatant was removed, adhered cells air dried and fixed with 5% v/v H_2O_2 for 5 min at room temperature. At the end of the incubation, wells were emptied and washed twice with PBS and blocked with 5% BSA. Purified anti-MUC1 nanobody (0.5 μg/well) was added next and incubated for 75 min at 0 °C. The wells were washed twice with PBS/0.1% v/v BSA and incubated with 100 μL of 1:5000 diluted anti-Cmyc-HRP for 1 h on ice. Procedures for substrate addition, colour development, stopping enzymatic reaction and final measurements are described in detail elsewhere [24]. An unrelated nanobody (anti-endoglin nanobody) and 4% MPBS were used as negative control.

2.8. Synthesis of Mal-PEG-PEI and nanobody-PEG-PEI conjugates

Bi-functional PEG (Mal-PEG-NHS) dissolved in 100 mM degassed phosphate buffer (pH 7.0) was reacted with branched PEI (25 kDa) at a molar ratio of 40:1 at room temperature for 2.5 h under nitrogen [31]. Unconjugated PEG was removed by gel-permeation chromatography using G-50 Sephadex eluting with degassed phosphate buffer at pH 5.0. The content of PEG substitution was determined by maleimide assay with Ellman reagent [32]. For coupling of nanobody to Mal-PEG-PEI, nanobody was first reduced in 2 mM Tris[2-carboxyethyl]phosphine (TCEP) for 2 h at room temperature. TCEP was removed by Amicon ultra filter centrifugation (10 kDa). Reduced nanobody was added to the Mal-PEG-PEI at a molar ratio of 30:1 at room temperature and allowed to react for 16 h under nitrogen. The reaction was quenched with 1.0 mM L-cysteine for 1 h at room temperature (this procedure was also used to obtain Cys-PEG-PEI conjugates). Nanobody (Nb)-PEG-PEI was concentrated by gel-permeation chromatography using a G-50 Sephadex column and finally dialyzed (M_w cut-off 20 kDa) against 150 mM NaCl, pH 7.0. The concentration of PEI in Cys-PEG-PEI and Nb-PEG-PEI conjugates was determined using a copper sulfate assay [33] and the amine concentration was measured by the TNBS assay [34]. The amount of nanobody was determined by UV spectrometry ($\varepsilon = 19{,}000\ M^{-1}\ cm^{-1}$) with background correction using a solution of Cys-PEG-PEI.

2.9. Polyplex formation

All complexes of DNA and conjugates were prepared freshly before use. Conjugate solutions (Nb-PEG-PEI or Cys-PEG-PEI) in serum free cell culture media (50 μL) were added to the DNA solutions [pCDNA-3HRE/2ERE-pMUC1-tBid (tBid construct) or RE1-RE1-RE1-pSyn-tBid or pCDNA3.1-Hygro$^+$-GFP (GFP construct)] in equal volumes at required N/P ratios, mixed by vortexing and incubated for 15 min before use. Polyplex size and electrophoretic mobility were measured with Zetasizer 3000 HSA (Malvern Instruments, Malvern, UK) as described earlier [16,35]. DNA complexation and condensation were also followed by agarose gel (1% gel) retardation assay in the presence of ethidium bromide [18].

2.10. Polyplex binding, cell transfection and gene expression

MCF7, SKBR3, T47D, A431 and NIH3T3 cell lines (4×10^4 cells) were seeded and cultured in 48 well plates 3–4 days prior to transfection. Before transfection, cells were kept in antibiotic free media containing 0.5% of FCS for 2 h. Designated polyplexes (N/P = 5.7 corresponding to 0.5 μg DNA) were added next and at 4 h post transfection, the medium was replaced with fresh culture media. Gene expression was measured by real time (RT)-PCR at 16 h post transfection. The total RNA was extracted using total RNA isolation kit, NucleoSpin RNA II (Macherey-Nagel, Duren,

Germany). Equal amounts of RNA, from differentially treated and non-treated (control) cell lines were used for cDNA synthesis using M-MuLV reverse transcriptase (MBI, Fermentas, St. Leon-Rot, Germany) and 19 mer oligo-dT (Fermentas). The RT-PCR with a total volume of 20 μL consisted of 2X SYBR green RT-PCR Master Mix (Applied Biosystem, Foster City, CA), templates and t-Bid primers. Analysis of β-actin mRNA expression (as an internal control) was used to normalize the amount of template [4]. Cell viability was determined by direct cell counting using Trypan blue exclusion test [36].

Nanobody-tagged polyplex binding to cells was assessed by flow cytometry. Cells were incubated with designated polyplexes as above or 1% w/v BSA (as control) for 30 min at 4 °C. Afterwards, cells were washed twice with 1% w/v BSA and incubated with ER-46 nanobody (10 μg/mL) for 35 min. Washing steps were repeated again and cells were resuspended in 200 μL PBS. This was followed by sequential addition of monoclonal anti-hemagglutinin and FITC conjugated rabbit anti-mouse (LifeSpan BioSciences). At the end of incubation time, cells were resuspended in 500 μL 1% paraformaldehyde (in PBS) and analyzed by flow cytometry (FACScan, BectonDickinson, Heidelberg, Germany). Results were statistically evaluated with Cell Quest (BectonDickinson) software. Monoclonal mouse isotype IgG1 was used to determine background immunostaining.

2.11. Qualitative caspase 3 activity determination

Caspase-3 activity was monitored at the same time as RT-PCR analysis using a commercially available caspase 3 ELISA kit (BD Pharmingen, San Diego, CA, USA) in accordance with the manufacturer's instruction.

3. Results and discussion

3.1. Isolation, over-expression, purification and characterization of anti-MUC1 nanobody

Phage panning was guided through the rising number of phages in steps of panning. The results of the polyclonal phage ELISA showed that the A_{450nm} difference was highest in the 4th and 5th rounds of panning. Among the 120 clones, the ER-46 clone was subsequently selected by ELISA against the MUC1 antigen and its nucleotide sequence was deposited in the GenBank database under accession number FJ799116. After sub-cloning into the pSJ expression vector, which allows for the expression of recombinant protein fused to the Cmyc-tag and six amino acids His-tag downstream of the cloning site, the ER46-28 clone was selected as the final clone for large scale nanobody production. The anti-MUC1 nanobody was purified from IMAC column (at an imidazole concentration of 200 mM) and the purification was confirmed using electrophoresis and immunoblotting (Fig. 1a–c). Under non-reducing conditions the IMAC purified nanobody can form dimers (Fig. 1a) since it bears an unpaired cysteine at the C-terminal, but a single band of 18 kDa (Fig. 1b) is observable under reducing conditions (Fig. 1b). The best conditions (IPTG 0.8 mM, 28 °C and 72 h) were chosen for large scale nanobody production. Subsequently, we used TCEP to reduce the nanobody for conjugation to the distal end of the reactive PEG in PEG-PEI conjugates.

The reactivity of ER46-28 with purified MUC1 antigen and a synthetic mucin peptide, containing two repeats of the APDTR epitope of the MUC1 antigen backbone exposed in cancer, was confirmed by both ELISA and radioimmunoassay and no cross-reactivity with non-specific proteins was detectable (Fig. 1d and e). The results of the affinity determination yielded a *Ka* value of $2.8\times10^{10}\ M^{-1}$ for the purified anti-MUC1 nanobody. Cell ELISA analysis further confirmed that the purified anti-MUC1 nanobody binds effectively to human cancerous cell lines expressing high levels of MUC1 antigen, whereas no significant binding occurs to non-MUC1 expressing cells (e.g., NIH3T3 cell line), Fig. 1f.

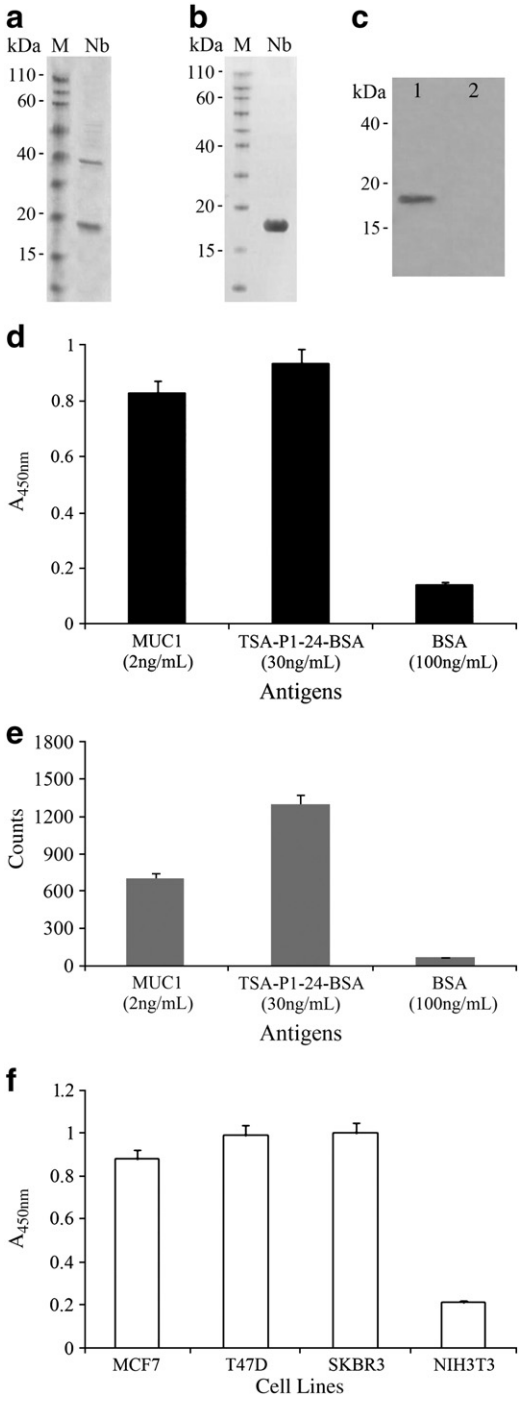

Fig. 1. Purification, characterization and reactivity of ER46-28 anti-MUC1 nanobody. Panels a–c represent non-reducing PAGE, SDS-PAGE and the immunoblot of the SDS-PAGE purified nanobody, respectively. In the immunoblot (c), lane 1 shows the purified nanobody and lane 2 corresponds to a negative control (extract of non-transformed bacterial cells). In (d) and (e) nanobody reactivity was determined by ELISA and radioimmunoassay, respectively. Panel (f) represents cell ELISA analysis of the binding of purified nanobody to cell lines expressing the MUC1 antigen. A_{450nm} values following anti-endoglin nanobody treatment were less than 0.2 absorbance units in all cases (not shown).

3.2. Preparation and characterization of nanobody tagged polyplexes

We used an established procedure [31] for coupling of a bi-functional PEG_{3500} to branched 25 kDa PEI. The procedures yielded conjugates containing on average 16 PEG_{3500} per PEI molecule based on maleimide assay with Ellman reagent and PEI determination with

the copper sulfate assay. The purified nanobody was next reduced with TCEP and coupled to the maleimide moiety at the distal end of the PEG molecules in PEG-PEI conjugates. This yielded on average 8.7 nanobody molecules per Mal-PEG-PEI molecule at a molar ratio of 30:1 nanobody to maleimide-PEG. Higher ratios of nanobody to maleimide-PEG did not increase the coupling efficiency (not shown). Since not all reactive PEG molecules are coupled to nanobodies, this may suggest hydrolysis of a fraction of maleimide into the non-reactive maleamic acid.

Next, polyplexes from Nb-PEG-PEI or PEG-PEI (since the distal end of the reactive PEG in PEG-PEI was quenched with cysteine the final product is referred to as Cys-PEG-PEI) conjugates and plasmid DNA were prepared at N/P of 3, 5.7 and 12. At all tested N/P's polyplexes exhibited hydrodynamic size ranges of 130–140 nm, but differed in zeta potential (ζ) values. For example, at the N/P of 5.7 the hydrodynamic sizes were 132 ± 20 nm and 140 ± 51 nm for Nb-PEG-PEI and Cys-PEG-PEI polyplexes, respectively. The corresponding ζ values were $+6$ mV and -3 mV for Nb-PEG-PEI and Cys-PEG-PEI polyplexes, respectively, confirming effective PEG shielding of PEI, since in the absence of PEGylation ζ values of polyplexes formed between PEI and DNA were highly positive ($+28$ mV). No significant differences in ζ values were observed when N/P was increased from 5.7 to 12 and regardless of the polyplex type. On the other hand, at N/P of 3 polyplexes exhibited more positive ζ values (10–12 mV) compared with N/P of 5.7, indicating poor PEG shielding.

The physicochemical properties of the engineered polyplexes at N/P of 5.7 make them highly favourable for transfection procedures. Indeed, agarose gel retardation assays demonstrated complete retardation of DNA with both types of PEGylated polyplexes indicating that complete DNA complexation was achieved at the N/P ratio of 5.7 (Fig. 2a) and this is in agreement with the earlier suggestion that PEGylated PEI's can compact DNA efficiently [18]. Due to sufficient PEGylation, constructed polyplexes expressed a surface charge close to neutrality. PEG shielding is expected to dramatically suppress direct PEI-mediated polyplex interaction with the plasma membrane (the cationic charge effect) [18,19], thus allowing for assessment of nanobody mediated binding to MUC1 antigen on the cell surface and subsequent plasmid delivery, release and tBid expression. This notion is further supported by the observation that conjugated anti-MUC1 nanobodies in polyplexes remain functionally active and efficiently recognize their designated targets on the cell surface as determined by competition assays (Fig. 2b). Therefore, the plasmid DNA seems to interact with the PEI domain without steric interference from conjugated PEG chains and form polyplexes with hydrodynamic size distributions amenable for receptor mediated binding and subsequent internalization.

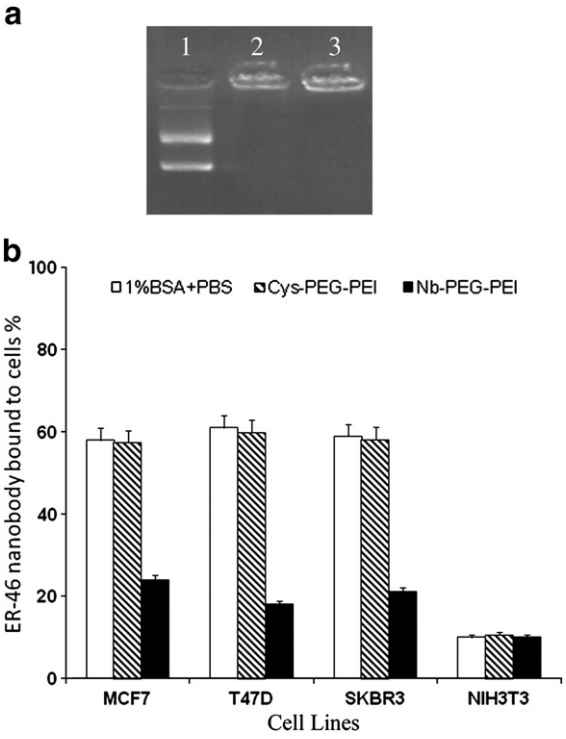

Fig. 2. Functional activities and properties of engineered polyplexes. Panel (a) shows agarose gel electrophoresis of plasmid DNA and polyplexes (N/P = 5.7); lane 1 = pCDNA-3HRE/2ERE-pMUC1-tBid (tBid construct), lane 2 = Cys-PEG-PEI/tBid construct polyplex and lane 3 = Nb-PEG-PEI/tBid construct polyplex. Panel (b) represents flow cytometric analysis of ER-46 nanobody to cells after pre-treatment with control and nanobody-tagged polyplex (N/P = 5.7). The extent of ER-46 nanobody binding inhibition was similar after preincubation of cells with polyplexes of N/P = 12.

3.3. Cancer cell transfection, tBid mRNA expression, cell death and caspase 3 activity analysis

Recently we demonstrated the killing efficacy of the pCDNA-3HRE/2ERE-pMUC1-tBid vector system (the tBid construct) following transfection of MUC1 over-expressing cancer cells by both electroporation and Lipofectamine (a cell non-specific cationic transfectant) [4]. Here, we extended our studies with a nanobody targeting approach for cell selective and safe delivery of the tBid transgene. The results in Fig. 3a show that both untreated MUC1 over-expressing cells and control cell lines have low levels of endogenous Bid/tBid expression, as determined by RT-PCR, and high cell viability is indicated. Following treatment of all cell types with the Cys-PEG-PEI polyplexes containing the lethal gene, the extent of Bid/tBid expression was increased slightly when compared with control treatments, but this had no effect on cell death (Fig. 3b). This observation may be related to the presence of small quantities of native or poorly PEGylated PEI molecules in this preparation that following internalization induces a 'gene signature' resulting in up-regulation of pro-apoptotic genes such as Bid [15]. However, an increase in Bid mRNA level may not necessarily lead to an increase in Bid expression, subsequent cleavage to tBid and cell death. On the other hand, with anti-MUC1 tagged polyplexes carrying the lethal gene, but strictly under the control of MUC1 promoter, Bid/tBid expression was highly prominent in MUC1 over-expressing cells (Fig. 3c). This was further associated with a dramatic increase in cell death and, remarkably, in the absence of hypoxic conditions and oestrogen treatment. The engineered system, as expected, showed poor specificity for cells with low/limited MUC1 expression (A431) and non MUC1-expressing cells, since Bid/tBid expression level and cell viability was comparable with respective control treatments. Notably, with Nb-PEG-PEI polyplexes carrying tBid gene but under the control of synapsin I promoter, which is specific for the central nervous system transcriptional targeting [26], Bid/tBid expression level and the extent of cell death in both MUC1-expressing and control cell lines remained comparable with respective control treatments (Fig. 3d). Similarly, Nb-PEG-PEI polyplexes carrying the GFP gene did not induce elevated Bid/tBid expression compared with the endogenous levels and cell viability also remained comparable with control treatments (Fig. 3e). The transfection efficacy of this vector for GFP expression was 35% in MUC1 expressing cells based on GFP fluorescence measurement; while the percentage of GFP positive cells with the control conjugates (Cys-PEG-PEI polyplexes carrying GFP gene) was 2–3%. These observations further confirm that nanobody binding to MUC1 has no indirect effect on cell death. Therefore, our data collectively suggest that the effective MUC1-positive cell destruction is the result of combined nanobody mediated tBid transgene delivery and transcriptional targeting exclusively based on the MUC1 promoter. This statement is further supported by observations that cell treatment with non-PEGylated PEI or transfection with PEI polyplexes containing the tBid gene (Fig. 3f

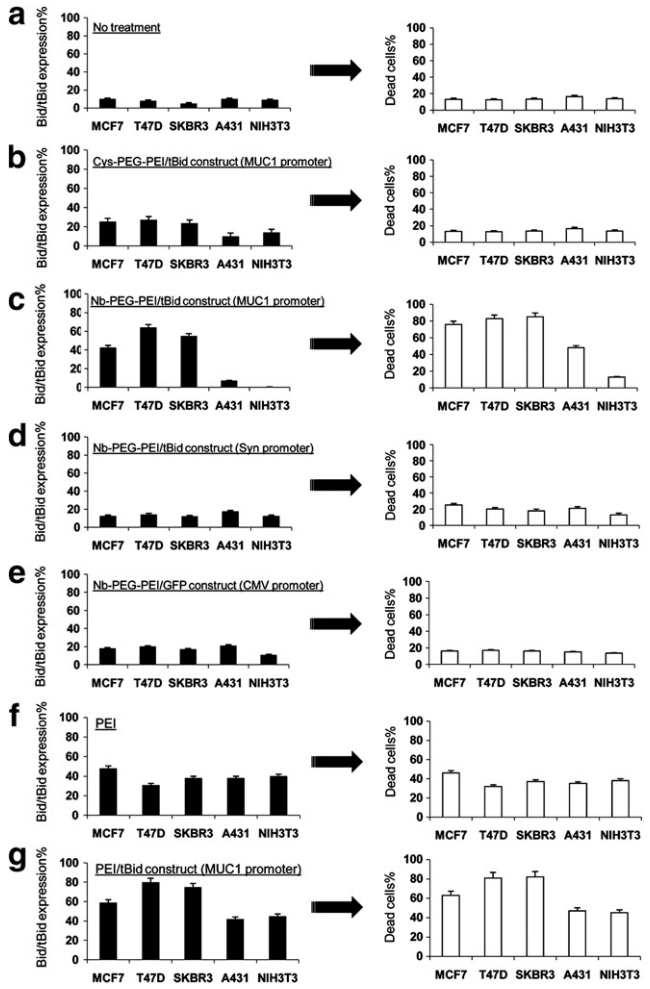

Fig. 3. Assessment of Bid/tBid mRNA expression and cell death following treatment with different engineered polyplexes. Panel (a) represents no treatment, panel (b) shows responses to treatment with Cys-PEG-PEI/tBid construct polyplexes, panel (c) demonstrates the effect of nanobody (Nb)-PEG-PEI/tBid construct polyplexes under the control of MUC1 promoter, panel (d) shows the effect of the same polyplex but under the control of synpasin I (Syn) promoter, which is a central nervous system specific promoter, panel (e) is indicative of treatment responses to nanobody-tagged polyplexes carrying GFP gene under the control of CMV promoter, and panels (f) and (g) indicative of treatments with PEI alone and PEI constructs carrying tBid gene under the control of MUC1 promoter, respectively. All tests were performed in triplicates. Analysis of Bid/tBid mRNA expression was done by RT-PCR after 16 h and expression levels are presented after normalization against β-actin mRNA levels. Analysis of cell death in transfected and non-transfected cells was done by Trypan blue exclusion test.

and g) show increased Bid/tBid expression as well as cell death, where the results are most prominent with the latter and in the case of MUC1 expressing cell lines. For A431(with low/limited MUC1 expression) and NIH3T3 cell line (non-MUC1 expressing cell line) the extent of Bid mRNA expression and cell death remains similar with both treatment regimens. This corresponds well to the previously established role of PEI, which in a concentration and time-dependent manner can induce both apoptosis and necrosis [16]. The results in Fig. 4 further confirm that treatment with non-PEGylated PEI enhances caspase 3 activity in all cell lines (with the exception of MCF7 cells).

The increased executioner caspase 3 activity in MUC1-positive cell lines (with the exception of MCF7 cells) following treatment with Nb-PEG-PEI polyplexes carrying the tBid transgene (Fig. 4) further attests to the initiation of apoptosis. This indicates that following internalization, the engineered nanobody-tagged polyplexes, in spite of being PEGylated, are still capable of releasing plasmid cargos into the cytoplasm (presumably due to the operation of 'proton sponge' hypothesis or other recently suggested mechanisms [15,37]) and subsequently achieving high specificity of tBid gene expression under the control of the MUC1 promoter. However, the plasmid releasing mechanism may partly be related to the presence of small qualities of high molecular weight non-PEGylated (or poorly PEGylated) PEI molecules in the polyplexes [38,39]. We were not able to demonstrate elevated caspase 3 activity in all tested cell lines following challenge with nanobody-tagged PEGylated polyplexes carrying the GFP gene or the tBid gene under the control of the synapsin I promoter (not shown), thus eliminating a significant role for PEI-mediated initiation of apoptosis either directly through the mitochondrion [11], or indirectly through other pathways, during the time-frame of these experiments. This also attests that PEGylation can dramatically overcome the apoptotic effect of PEI at least with the quantities used in these experiments and the possible presence of free PEI in polyplexes must be at concentrations below the level that is required to induce apoptosis and/or necrosis. Therefore the procedures used overcomes PEI-mediated apoptotic and necrotic cell death, which is advantageous for *in vivo* transcriptional targeting, as this will minimize (or eliminate) non-targeted cell damage. The high efficiency of tBid-mediated apoptotic cancer cell killing also arises from the fact that it does not require post-translational modifications.

MCF7 cells are deficient in caspase 3 expression because of a deletion mutation in exon 3 in the caspase 3 gene [40]. This raises an interesting question as how nanobody-tagged PEGylated polyplexes carrying the killer gene can induce cell death in caspase 3 deficient MCF7 cells. Our observations, however, are in line with recently reported suggestions that caspase 8-mediated Bid cleavage triggers cytochrome *c*-mediated apoptosis in MCF7 cells [41]. Furthermore, treatment of MCF7 cells with Bax-overexpression vectors has also been shown to induce caspase 8 activation and cell death [42]. Since these treatments in MCF7 cells further resulted in caspase 6 activation, which is responsible for the digestion of nuclear substrates lamin A and B [43] and accounts for the nuclear morphological changes during apoptosis, the existence of alternative mechanisms that act in place of caspase 3 and instead leads to caspase 6 activation can be hypothesized.

4. Conclusions

In summary, we have isolated an anti-MUC1 nanobody with high specificity for a MUC1 antigen and used this to engineer PEGylated PEI conjugates for successful compaction of the tBid killer gene and its selective delivery into MUC1 expressing cell lines. Our data provides a powerful proof of concept in combining nanobody-based targeting with transcriptional targeting as a safe way to deliver transgenes to specific cells; this overcomes PEI-mediated cellular toxicity (due to low PEI concentrations used), which is also important when considering the cytotoxicity associated with cationic polyplexes and lipoplexes in general. Here, targeting is exclusively nanobody-mediated and PEI-plasma membrane interactions do not significantly contribute to polyplex internalization and tBid expression. The choice of the targeting ligand (nanobody) has other advantages; it not only has a small size and expresses favourable physicochemical characteristics amenable for conjugation, but also overcomes some of the problems frequently encountered with administration of monoclonal antibody-tagged nanoparticles/nanoconstructs (e.g., Fc-mediated clearance). Nanobody monovalency reduces its binding strength because of the reduction in avidity effects. However, this is overcome by high nanobody density on the surface of the polyplexes.

Acknowledgements

This work was partly supported by the Nanotechnology Committee of Tarbiat Modares University (to F. Rahbarizadeh) and Facualty of Medical Sciences of Tarbiat Modares University for E. Sadeqzadeh thesis and in part by the Danish Agency for Science, Technology and Innovation (Det Frie Forskningsråd for Teknologi og Produktion, reference 274-08-0534, and Det Strategiske Forskningsråd, reference 09-065746/DSF, to SMM).

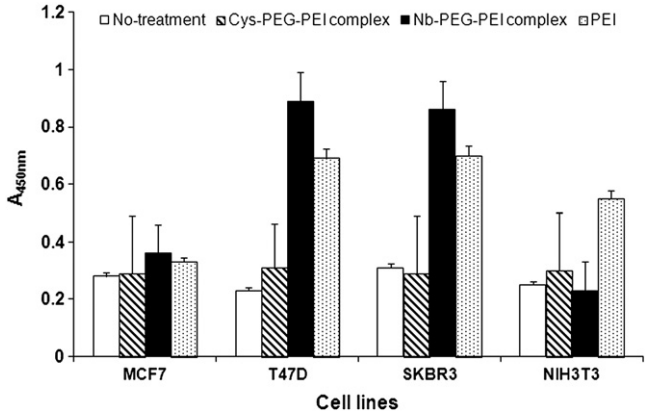

Fig. 4. Caspase 3 activity in cells following transfection with different tBid transgene carrying engineered polyplexes and treatment with free PEI. Cys-PEG-PEI/tBid construct and Nb-PEG-PEI/tBid construct polyplexes under the control of MUC1 promoter were used. Caspase 3 determination was performed in duplicate and the results are average of optical density (450 nm) for each cell line ± SEM.

References

[1] J.J. Rojas, S. Guedan, P.F. Searle, J. Martinez-Quintanilla, R. Gil-Hoyos, F. Alcayaga-Miranda, M. Cascallo, R. Alemany, Minimal RB-responsive E1A promoter modification to attain potency, selectivity, and transgene-arming capacity in oncolytic adenoviruses, Mol. Ther. 18 (2010) 1960–1971.

[2] P.H. Kim, T.I. Kim, J.W. Yockman, S.W. Kim, C.O. Yun, The effect of surface modification of adenovirus with an arginine-grafted bioreducible polymer on transduction efficiency and immunogenicity in cancer gene therapy, Biomaterials 31 (2010) 1865–1874.

[3] T. Robson, D.G. Hirst, Transcriptional targeting in cancer gene therapy, J. Biomed. Biotechnol. 2003 (2003) 110–137.

[4] S. Farokhimanesh, F. Rahbarizadeh, M.J. Rasaee, A. Kamali, B. Mashkani, Hybrid promoters directed tBid gene expression to breast cancer cells by transcriptional targeting, Biotechnol. Prog. 26 (2010) 505–511.

[5] I. Kazhdan, L. Long, R. Montellano, D.A. Cavazos, R.A. Marciniak, Targeted gene therapy for breast cancer with truncated Bid, Cancer Gene Ther. 13 (2006) 141–149.

[6] S.C. Ruffolo, D.G. Breckenridge, M. Nguyen, I.S. Goping, A. Gross, S.J. Korsmeyer, H. Li, J. Yuan, G.C. Shore, BID-dependent and BID-independent pathways for BAX insertion into mitochondria, Cell Death Differ. 7 (2000) 1101–1108.

[7] M.C. Wei, W.X. Zong, E.H. Cheng, T. Lindsten, V. Panoutsakopoulou, A.J. Ross, K.A. Roth, G.R. MacGregor, C.B. Thompson, S.J. Korsmeyer, Proapoptotic BAX and BAK: a requisite gateway to mitochondrial dysfunction and death, Science 292 (2001) 727–730.

[8] X.M. Yin, Bid, a BH3-only multi-functional molecule, is at the cross road of life and death, Gene 369 (2006) 7–19.

[9] A. Gross, X.M. Yin, K. Wang, M.C. Wei, J. Jockel, C. Milliman, H. Erdjument-Bromage, P. Tempst, S.J. Korsmeyer, Caspase cleaved BID targets mitochondria and is required for cytochrome c release, while BCL-XL prevents this release but not tumor necrosis factor-R1/Fas death, J. Biol. Chem. 274 (1999) 1156–1163.

[10] Y. Zaltsman, L. Shachnai, N. Yivgi-Ohana, M. Schwarz, M. Maryanovich, R.H. Houtkooper, F.M. Vaz, F. De Leonardis, G. Fiermonte, F. Palmieri, B. Gillissen, P.T. Daniel, E. Jimenez, S. Walsh, C.M. Koehler, S.S. Roy, L. Walter, G. Hajnoczky, A. Gross, MTCH2/MIMP is a major facilitator of tBID recruitment to mitochondria, Nat. Cell Biol. 12 (2010) 553–562.

[11] S.J. Korsmeyer, M.C. Wei, M. Saito, S. Weiler, K.J. Oh, P.H. Schlesinger, Pro-apoptotic cascade activates BID, which oligomerizes BAK or BAX into pores that result in the release of cytochrome c, Cell Death Differ. 7 (2000) 1166–1173.

[12] P.L. Devine, G.W. Birrell, R.H. Whitehead, H. Harada, P.X. Xing, I.F. McKenzie, Expression of MUC1 and MUC2 mucins by human tumor cell lines, Tumour Biol. 13 (1992) 268–277.

[13] S. Duraisamy, T. Kufe, S. Ramasamy, D. Kufe, Evolution of the human MUC1 oncoprotein, Int. J. Oncol. 31 (2007) 671–677.

[14] M. Neu, D. Fischer, T. Kissel, Recent advances in rational gene transfer vector design based on poly(ethylene imine) and its derivatives, J. Gene Med. 7 (2005) 992–1009.

[15] L. Parhamifar, A.K. Larsen, A.C. Hunter, T.L. Andresen, S.M. Moghimi, Polycation cytotoxicity: a delicate matter for nucleic acid therapy-focus on polyethylenimine, Soft Matter 6 (2010) 4001–4009.

[16] S.M. Moghimi, P. Symonds, J.C. Murray, A.C. Hunter, G. Debska, A. Szewczyk, A two-stage poly(ethylenimine)-mediated cytotoxicity: implications for gene transfer/therapy, Mol. Ther. 11 (2005) 990–995.

[17] A.C. Hunter, S.M. Moghimi, Cationic carriers of genetic material and cell death: a mitochondrial tale, Biochim. Biophys. Acta-Bioenergetics 1797 (2010) 1203–1209.

[18] H. Petersen, P.M. Fechner, A.L. Martin, K. Kunath, S. Stolnik, C.J. Roberts, D. Fischer, M.C. Davies, T. Kissel, Polyethylenimine-graft-poly(ethylene glycol) copolymers: Influence of copolymer block structure on DNA complexation and biological activities as gene delivery system, Bioconjug. Chem. 13 (2002) 845–854.

[19] T. Merdan, J. Callahan, H. Petersen, K. Kunath, U. Bakowsky, P. Kopeckova, T. Kissel, J. Kopecek, Pegylated polyethylenimine-Fab' antibody fragment conjugates for targeted gene delivery to human ovarian carcinoma cells, Bioconjug. Chem. 14 (2003) 989–996.

[20] S.M. Moghimi, A.C. Hunter, J.C. Murray, Long-circulating and target-specific nanoparticles: theory to practice, Pharmacol. Rev. 53 (2001) 283–318.

[21] T. Merdan, K. Kunath, H. Petersen, U. Bakowsky, K.H. Voigt, J. Kopecek, T. Kissel, PEGylation of poly(ethylene imine) affects stability of complexes with plasmid DNA under in vivo conditions in a dose-dependent manner after intravenous injection into mice, Bioconjug. Chem. 16 (2005) 785–792.

[22] C. Hamers-Casterman, T. Atarhouch, S. Muyldermans, G. Robinson, C. Hamers, E.B. Songa, N. Bendahman, R. Hamers, Naturally occurring antibodies devoid of light chains, Nature 363 (1993) 446–448.

[23] P. Holliger, P.J. Hudson, Engineered antibody fragments and the rise of single domains, Nat. Biotechnol. 23 (2005) 1126–1136.

[24] F. Rahbarizadeh, M.J. Rasaee, M. Forouzandeh Moghadam, A.A. Allameh, E. Sadroddiny, Production of novel recombinant single-domain antibodies against tandem repeat region of MUC1 mucin, Hybrid. Hybridomics 23 (2004) 151–159.

[25] F.G. Hanisch, T.R. Stadie, F. Deutzmann, J. Peter-Katalinic, MUC1 glycoforms in breast cancer–cell line T47D as a model for carcinoma-associated alterations of 0-glycosylation, Eur. J. Biochem. 236 (1996) 318–327.

[26] G. Thiel, M. Lietz, M. Cramer, Biological activity and modular structure of RE-1-silencing transcription factor (REST), a repressor of neuronal genes, J. Biol. Chem. 273 (1998) 26891–26899.

[27] D. Ahmadvand, M.J. Rasaee, F. Rahbarizadeh, R.E. Kontermann, F. Sheikholislami, Cell selection and characterization of a novel human endothelial cell specific nanobody, Mol. Immunol. 46 (2009) 1814–1823.

[28] M. Arbabi Ghahroudi, A. Desmyter, L. Wyns, R. Hamers, S. Muyldermans, Selection and identification of single domain antibody fragments from camel heavy-chain antibodies, FEBS Lett. 414 (1997) 521–526.

[29] M.M. Bradford, A rapid and sensitive method for the quantitation of microgram quantities of protein utilizing the principle of protein-dye binding, Anal. Biochem. 72 (1976) 248–254.

[30] J.D. Beatty, B.G. Beatty, W.G. Vlahos, Measurement of monoclonal antibody affinity by non-competitive enzyme immunoassay, J. Immunol. Methods 100 (1987) 173–179.

[31] S. Zhang, C. Kucharski, M.R. Doschak, W. Sebald, H. Uludag, Polyethylenimine-PEG coated albumin nanoparticles for BMP-2 delivery, Biomaterials 31 (2010) 952–963.

[32] G.L. Ellman, Tissue sulfhydryl groups, Arch. Biochem. Biophys. 82 (1959) 70–77.

[33] A. von Harpe, H. Petersen, Y. Li, T. Kissel, Characterization of commercially available and synthesized polyethylenimines for gene delivery, J. Control. Release 69 (2000) 309–322.

[34] J. Bullock, S. Chowdhury, A. Severdia, J. Sweeney, D. Johnston, L. Pachla, Comparison of results of various methods used to determine the extent of modification of methoxy polyethylene glycol 5000-modified bovine cupri-zinc superoxide dismutase, Anal. Biochem. 254 (1997) 254–262.

[35] P. Symonds, J.C. Murray, A.C. Hunter, G. Debska, A. Szewczyk, S.M. Moghimi, Low and high molecular weight poly(L-lysine)s/poly(L-lysine)-DNA complexes initiate mitochondrial-mediated apoptosis differently, FEBS Lett. 579 (2005) 6191–6198.

[36] B.C. Guo, Y.H. Xu, Bcl-2 over-expression and activation of protein kinase C suppress the trail-induced apoptosis in Jurkat T cells, Cell Res. 11 (2001) 101–106.

[37] J.P. Behr, The Proton Sponge: a trick to enter cells the viruses did not exploit, Chimia 51 (1997) 34–36.

[38] J.P. Clamme, J. Azoulay, Y. Mely, Monitoring of the formation and dissociation of polyethylenimine/DNA complexes by two photon fluorescence correlation spectroscopy, Biophys. J. 84 (2003) 1960–1968.

[39] J.P. Clamme, G. Krishnamoorthy, Y. Mely, Intracellular dynamics of the gene delivery vehicle polyethylenimine during transfection: investigation by two-photon fluorescence correlation spectroscopy, Biochim. Biophys. Acta 1617 (2003) 52–61.

[40] R.U. Janicke, M.L. Sprengart, M.R. Wati, A.G. Porter, Caspase-3 is required for DNA fragmentation and morphological changes associated with apoptosis, J. Biol. Chem. 273 (1998) 9357–9360.

[41] D. Tang, J.M. Lahti, V.J. Kidd, Caspase-8 activation and bid cleavage contribute to MCF7 cellular execution in a caspase-3-dependent manner during staurosporine-mediated apoptosis, J. Biol. Chem. 275 (2000) 9303–9307.

[42] S. Kagawa, J. Gu, T. Honda, T.J. McDonnell, S.G. Swisher, J.A. Roth, B. Fang, Deficiency of caspase-3 in MCF7 cells blocks Bax-mediated nuclear fragmentation but not cell death, Clin. Cancer Res. 7 (2001) 1474–1480.

[43] B. Buendia, A. Santa-Maria, J.C. Courvalin, Caspase-dependent proteolysis of integral and peripheral proteins of nuclear membranes and nuclear pore complex proteins during apoptosis, J. Cell Sci. 112 (1999) 1743–1753.